

Letter

## A Comparison of AMSR-E/Aqua Snow Products with *in situ* Observations and MODIS Snow Cover Products in the Mackenzie River Basin, Canada

Jinjun Tong <sup>1,\*</sup> and Isabella Velicogna <sup>1,2</sup>

<sup>1</sup> Department of Earth System Science, University of California, Irvine, CA, 92697-3100, USA; E-Mail: [isabella.velicogna@gmail.com](mailto:isabella.velicogna@gmail.com)

<sup>2</sup> Jet Propulsion Laboratory, Pasadena, CA, 91109-8099, USA

\* Author to whom correspondence should be addressed; E-Mail: [jinjunt@uci.edu](mailto:jinjunt@uci.edu).

Received: 16 August 2010; in revised form: 1 September 2010 / Accepted: 25 September 2010 /

Published: 28 September 2010

---

**Abstract:** Since 2002, global snow water equivalent (SWE) estimates have been generated using Advanced Microwave Scanning Radiometer (AMSR-E)/Aqua data. Accurate estimates of SWE are important to improve monitoring and managing of water resources in specific regions. SWE and snow map product accuracy are functions of topography and of land cover type because landscape characteristics have a strong influence on redistribution and physical properties of snow cover, and influence the microwave properties of the surface. Here we evaluate the AMSR-E SWE and derived snow map products in the Mackenzie River Basin (MRB), Canada, which is characterized by complex topography and varying land cover types from tundra to boreal forest. We compare *in situ* snow depth observations and Moderate Resolution Imaging Spectroradiometer (MODIS) snow cover maps from January 2003 to December 2007 with passive microwave remotely sensed SWE from AMSR-E and derived snow cover maps. In the MRB the mean absolute error ranges from 12 mm in the early winter season to 50 mm in the late winter season and overestimations of snow cover maps based on a 1 mm threshold of AMSR-E SWE varies from 4% to 8%. The optimal threshold for AMSR-E SWE to classify the pixels as snow ranges from 6 mm to 9 mm. The overall accuracy of new snow cover maps from AMSR-E varies from 91% to 94% in different sub-basins in the MRB.

**Keywords:** snow water equivalent; snow cover extent; AMSR-E; MODIS; Mackenzie River Basin

---

## 1. Introduction

The spatial and temporal distribution of snow cover extent (SCE) and snow water equivalent (SWE) is a very important component of the hydrology of northern watersheds [1,2]. A significant decrease of snow during spring over North America and Eurasia, possibly related to global warming, has been observed recently [3]. Various remotely sensed snow data have been widely utilized for cold regions to explore the relationships between snow distribution, river discharge, and climate change [1,2,4,5-7]. The accuracy of remotely sensed snow products should be well understood and incorporated in any investigations using such data.

Microwave remote sensing provides direct measurements of SWE in a specific region, and allows also the generation of SCE maps. Although SCE maps can also be obtained from optical remote sensing observations, the advantage of the microwave data is that the signal is not affected by clouds, which was a large source of uncertainty for products derived from optical data. However, the process of generating SWE and SCE maps from microwave measurements is quite complex and requires many assumptions, and assessing the accuracy of microwave derived estimates is also important.

Previous studies have analyzed the accuracy of microwave remotely sensed SWE compared with *in situ* snow observations. Derksen *et al.* [8,9] compared Special Sensor Microwave Imager (SSM/I) SWE estimated by Environment Canada to *in situ* observation of SWE in Western Canada. Tekeli [10] evaluated the Advanced Microwave Scanning Radiometer (AMSR-E) daily L3 SWE data based on ground measurements from 2002 to 2003 in Eastern Turkey. The accuracy of the SWE estimates varies with different topography and land cover type of the study region. Therefore, in order to have a comprehensive understanding of the accuracy of microwave derived SWE estimates, it is necessary to examine the accuracy of the retrieval in different regions. Here we evaluate the accuracy of the SWE retrieval from AMSR-E L3 data in Northern America, more specifically in the Mackenzie River Basin (MRB), Western Canada. This region is characterized by a very different topography and snow process compared to Eastern Turkey, and represents a good validation for SWE estimate in the northern latitudes characterized by highly variable topography and combinations of different land cover, such as tundra and boreal forest.

Microwave remote sensing can not map the snow cover extent directly. Thus, snow pixels are first identified using a threshold for the remotely sensed SWE. In the Canadian Arctic, previous studies adopted a threshold of 1 mm of SWE to classify the pixels [11,12]. However, there is limited research on the optimal SWE thresholds for classifying snow in more complex terrains such as the mountainous forest areas in the sub-basins of the MRB. Furthermore, it is challenging to evaluate the SCE maps from microwave remote sense owing to the lack of the ground reference maps for the whole research area. Tong *et al.* [7] found that the optimal SWE thresholds of SSM/I for classifying snow in MRB ranges from 12 mm to 37 mm in the different sub-basins.

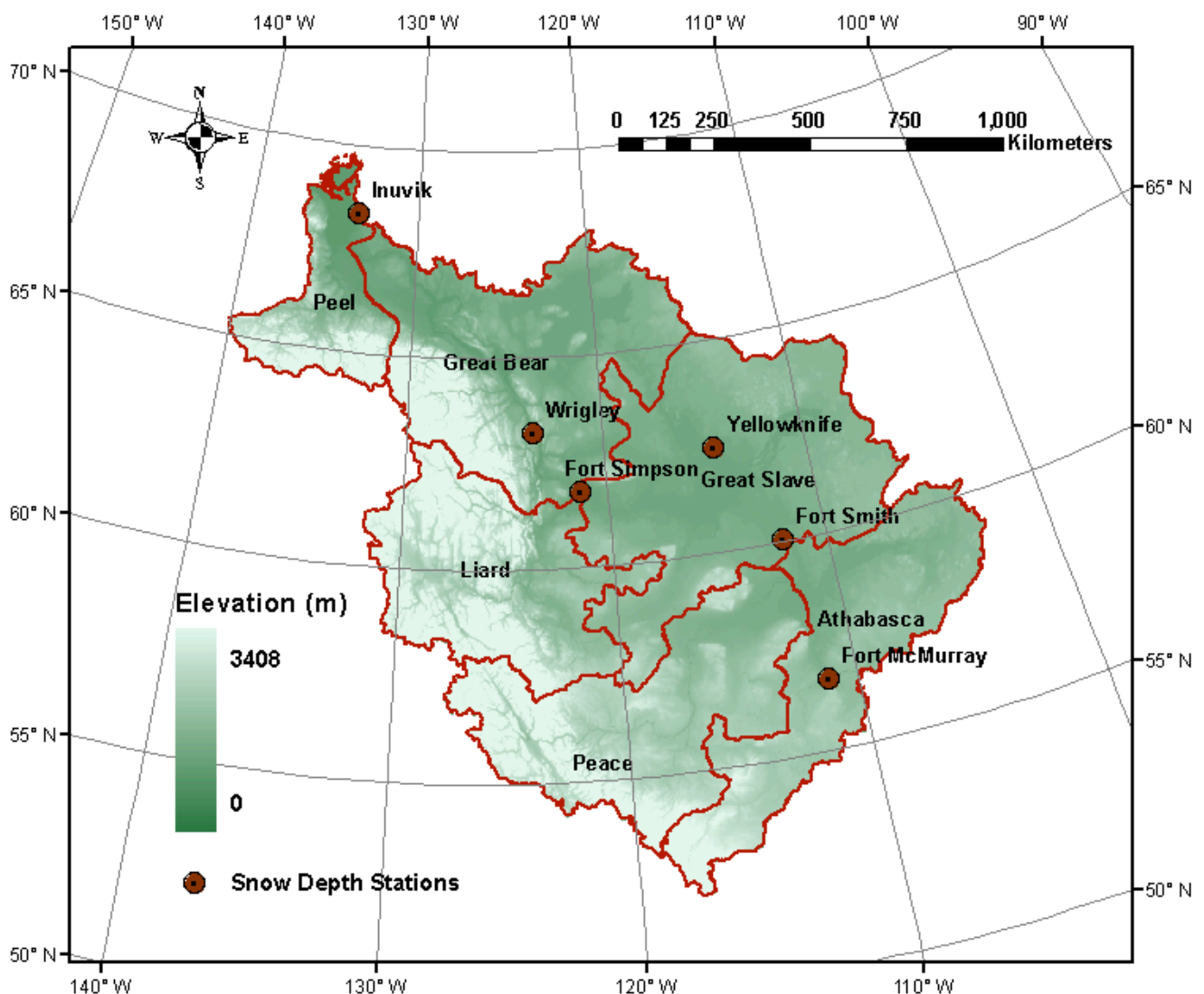
In this study, the AMSR-E derived daily L3 Global SWE Equal Area Scalable Earth Grid (EASE-Grid) products are evaluated based on *in situ* observations in different snow seasons in the MRB. In addition, Moderate Resolution Imaging Spectroradiometer (MODIS) SCE maps of the MRB are used to evaluate the AMSR-E SCE maps from AMSR-E. The agreements between the *in situ* and microwave remote sensed SWE are calculated. The optimal thresholds of SWE to produce the SCE

maps from AMSR-E SWE in different topography regions in MRB are determined based on the MODIS SCE maps, and we estimated the error introduced by the previously used thresholds.

## 2. Research Area

The MRB, which is located between 52°N–70°N, and 103°W–140°W, is the tenth largest river basin in the world, with an area covering about 1.8 million km<sup>2</sup>. The average elevation of the MRB is about 630 m with the highest elevation about 3,400 m in the west. There are six major sub-basins, the Peel, Great Bear, Liard, Great Slave, Peace, and Athabasca watersheds, which cover about 182, 598, 428, 668, 509, and 452 EASE-Grids of AMSR-E, respectively (Figure 1). The Peel and Great Bear basins are mainly covered by sparse forest or are open areas (94% and 80%, respectively), however, the other basins are mainly covered by coniferous and deciduous forest, varying from 50% to 75%. In the MRB as a whole, the open area, sparse vegetation, coniferous forests, and deciduous forests account for about 14%, 40%, 34%, and 12% in the MRB, respectively [7].

Figure 1. Study area map and location of the *in situ* snow observation stations of the Mackenzie River Basin (MRB). Digital elevation model is the Global Land One-kilometer Base Elevation (GLOBE) data set provided by the National Geophysical Data Center.



### 3. Data

#### 3.1. AMSR-E daily L3 Global SWE EASE-Grid Data

The AMSR-E is a multi-frequency, dual-polarized passive microwave radiometer launched on the NASA Aqua platform in May 2002. The AMSR-E has both horizontally and vertically polarized channels at 6.925, 10.65, 18.7, 23.8, 36.5 and 89 GHz (<http://www.ghcc.msfc.nasa.gov/AMSR/>). The retrieval of SWE is based on the brightness temperature (Tb) difference between channels owing to the attenuation of snow on the microwave radiation from the snow and underlying ground. The algorithms for SWE retrieval have been developed and improved in different regions [8,9,13,14]. The AMSR-E/Aqua L3 Global SWE EASE-Grid data with 25 km resolution from January 2003 to December 2007 were downloaded from the National Snow and Ice Data Center (NSIDC) in Boulder, Colorado (<ftp://sidacs.colorado.edu/pub/DATASETS/brightness-temperatures/polar-stereo/tools/>).

#### 3.2. MODIS Snow Products

MODIS, which has 36 discrete, narrow spectral bands from approximately 0.4 to 14.4  $\mu\text{m}$ , has been flying on the Terra spacecraft since 18 December 1999. The spatial resolution of MODIS bands range from 250 m to 1,000 m with a spectral resolution of 0.01  $\mu\text{m}$  to 0.05  $\mu\text{m}$  for the different bands. MODIS snow maps, which are mainly based on the SNOWMAP algorithm [15], are available at different resolutions and projections such as 500 m daily and 8-day data on a sinusoidal projection and 0.05°, 0.25° daily, 8-day, and monthly data on a latitude/longitude grid or the so-called climate-modeling grid (CMG). In this paper, version 005 (V5) of MODIS 8-day maximum snow extent (MOD10A2) from 2003 to 2007 were downloaded from National Snow and Ice Data Center (NSIDC; <http://nsidc.org>) and used to validate new snow cover products from AMSR-E L3 SWE data.

#### 3.3. In situ SWE Data

Six stations located in open, forested, or mixed land cover environments used by Derksen *et al.* [8] in the MRB were selected to evaluate the SWE of AMSR-E (Figure 1). The daily snow depth (SD) data were downloaded from Environment Canada ([http://www.climate.weatheroffice.ec.gc.ca/climateData/canada\\_e.html](http://www.climate.weatheroffice.ec.gc.ca/climateData/canada_e.html)). No SWE data were available for these stations. Previous comparison of snow survey SWE measurements and SWE estimates from snow depth data shows a moderately strong level of agreement with a correlation coefficient of 0.78 ( $p < 0.001$ ) between these datasets [8]. The SD data was converted into SWE by adopting the regionally and seasonally averaged snow density values provided by Brown [3] (with updates by Brown, personal communication, 2009).

### 4. Comparison between Datasets

#### 4.1. Comparison between SWE Datasets

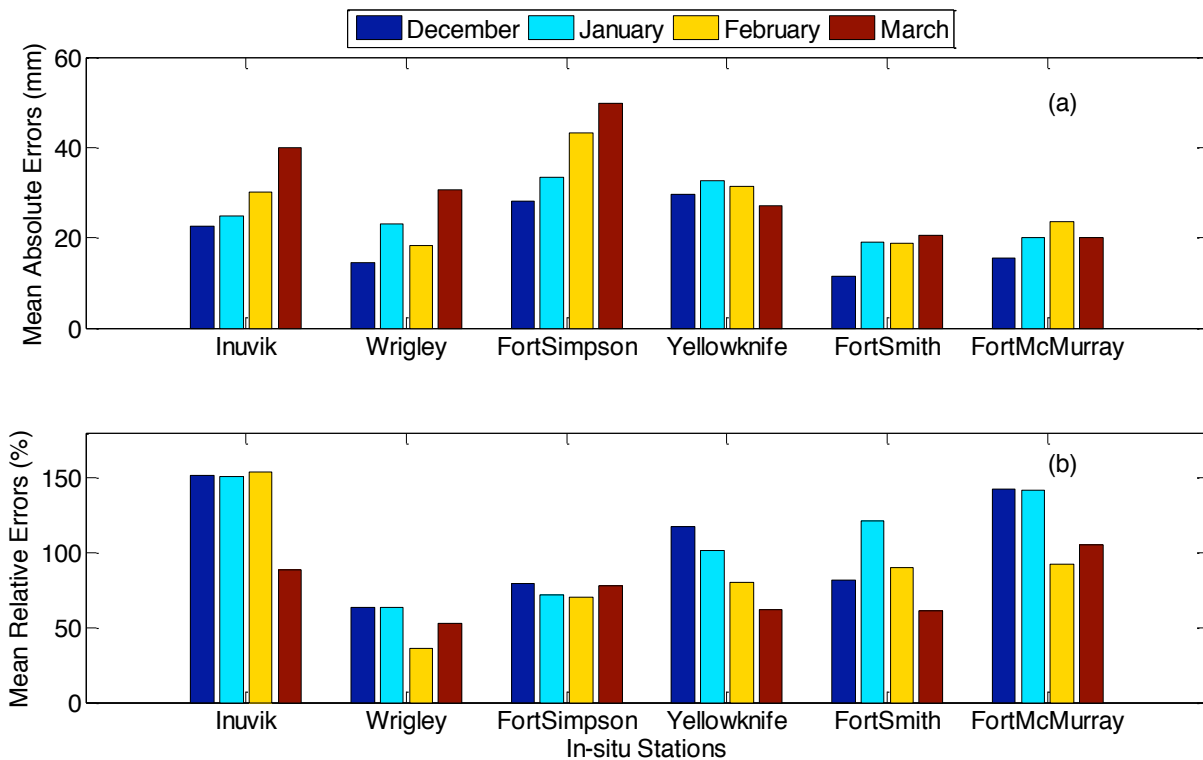
The quantitative comparison between the AMSR-E and *in situ* SWE is based on the mean absolute error (MAE) (Equation 1) and mean relative error (MRE) (Equation 2), which were adopted by Derksen *et al.* [8,9] to evaluate the agreement between SSM/I retrieved and *in situ* SWE.

$$MAE = \frac{\sum |SWE_{AMSR-E} - SWE_{insitu}|}{n} \tag{1}$$

$$MRE = \frac{\sum |SWE_{AMSR-E} - SWE_{insitu}| / SWE_{insitu}}{n} \tag{2}$$

where  $n$  is the total number of SWE pairs. Since the snow depth varies from lowest in early December to highest in later March, the mean absolute error and mean relative error in four different periods (December, January, February, and March) were calculated. Because of missing daily SD measurements in the *in situ* stations,  $n$  varies from 100 to 130. Figure 2 shows the mean absolute error and mean relative error for the six *in situ* SD stations. The absolute difference between microwave and *in situ* SWE increases as the winter season progresses. The mean absolute errors in December in all the stations are the lowest compared to later in the season; however, the mean relative error for all the stations is highest in December. The high mean relative error in December is related to the lower SWE during that period. The lowest mean absolute error is in December and is about 12 mm, while the highest mean absolute error is in March and is about 50 mm. The complex multi-layer snowpack in the later winter increases the difficulty for microwave retrieval of SWE, which likely resulted in the increased mean absolute error [8].

Figure 2. (a) The mean absolute errors and (b) mean relative errors of AMSR-E L3 snow water equivalent based on the *in situ* snow depth observations in the Mackenzie River Basin averaged over winter seasons from January 2003 to December 2007.



#### 4.2. Comparison between AMSR-E and MODIS Snow Cover

A threshold  $k$  for SWE is defined to produce snow cover maps from AMSR-E retrieved SWE. To determine the optimal threshold, 8-day snow cover maps from AMSR-E, which cover the same

temporal scale as the MOD10A2 data, were produced based on different thresholds for AMSR-E retrieved SWE. In every 8-day period, as long as SWE of a given pixel of one day is greater than the threshold, the pixel is classified as snow; otherwise, the pixel is classified as not snow.

Owing to high accuracy compared to the *in situ* observations in different regions, the MOD10A2 snow cover products were adopted as a reference data set to evaluate the snow cover products from AMSR-E [4-6,16,17]. However, the different spatial resolutions of AMSR-E and MODIS and the cloud pixels in the MOD10A2 need to be addressed before any comparison. A spatial filtered method, which substitutes a cloudy pixel with the majority type in the 8 surrounding pixels, is used to decrease the cloud coverage of MOD10A2 [5,6]. The spatially filtered snow cover maps are referred to as SF hereafter. In order to compare the AMSR-E snow products with MODIS snow products, which have 25 km and 500 m spatial resolution, respectively, the SF products were reclassified into new snow cover maps with 25 km resolution. For the 2,500 SF pixels in a 25 km EASE-Grid of AMSR-E, the relative proportion of snow, not snow, and cloud are compared and the EASE-Grid is classified as the class with the highest proportion. In this way, the reference 8-day snow cover maps with 25 km resolution covering the period 2003–2007 were produced.

The overall accuracy, under-estimation error, and over-estimation error methods used by Tong *et al.* [5,6] and Parajka and Blöschl [17] are adopted to evaluate the snow maps from AMSR-E. For a given pixel, there are four possible outcomes in a comparison of snow maps from SF with AMSR-E (Table 1). The overall accuracy, under-estimation error, and over-estimation error of AMSR-E snow products are calculated by Equations 3–5.

$$\text{Overall accuracy} = \frac{a + d}{a + b + c + d} \quad (3)$$

$$\text{Under-estimation error} = \frac{b}{a + b + c + d} \quad (4)$$

$$\text{Over-estimation error} = \frac{c}{a + b + c + d} \quad (5)$$

where terms *a*, *b*, *c* and *d* are defined in Table 1. For a given pixel, there are two different time series of snow condition including snow maps from AMSR-E and SF. All overall accuracy, under-estimation error, and over-estimation errors are based only on the days when SF snow products are not labeled on cloud. Then for every given threshold of SWE, the average overall accuracy, under-estimate error, and over-estimate error of snow maps from AMSR-E in every sub-basin were calculated. The water bodies in the MRB were not included in the comparison.

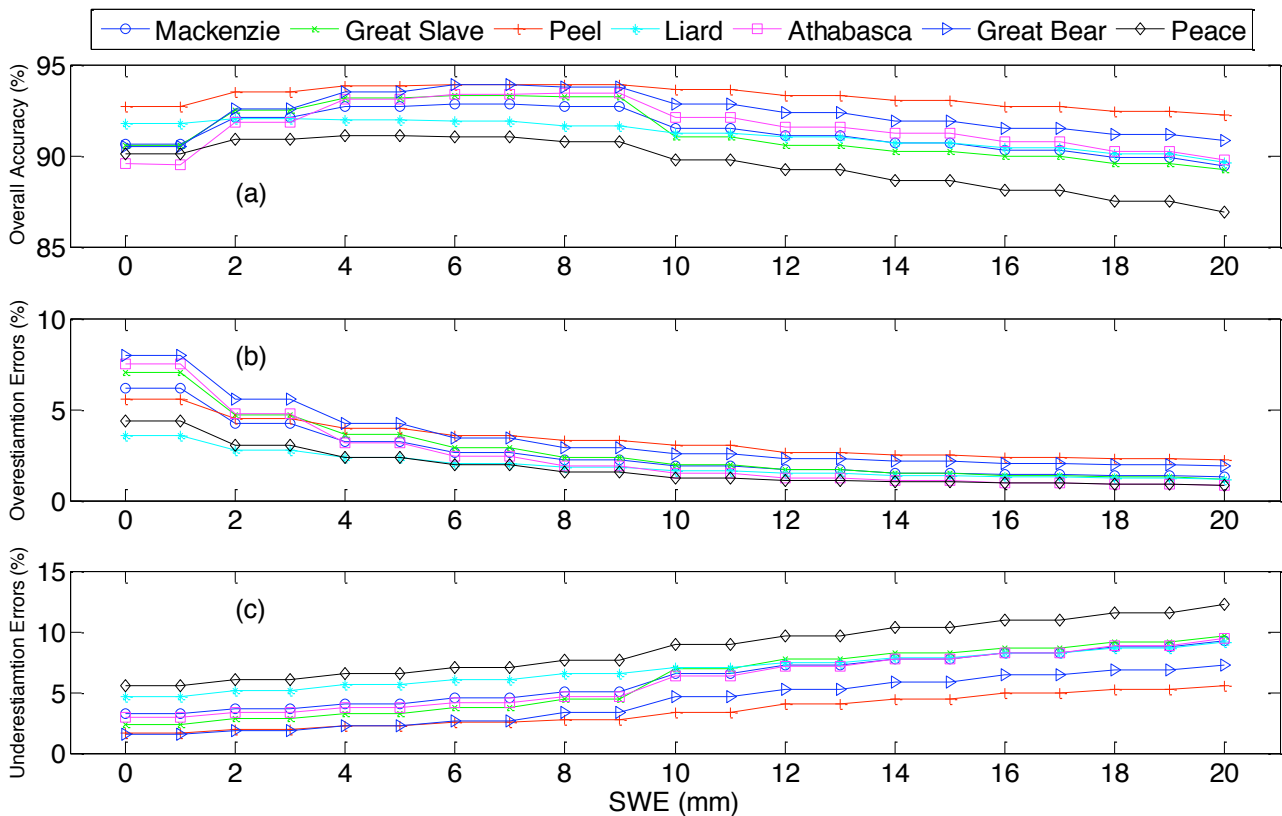
Table 1. Confusion Matrix for snow cover maps from AMSR-E and MODIS.

	AMSR-E	Snow	Not Snow
MODIS (Reference Data)			
Snow		a	b
Not Snow		c	d

Snow maps from AMSR-E based on thresholds ranging from 0 mm to 20 mm were produced. The average overall accuracy, under-estimate error, and over-estimation error for different sub-basins in the

MRB with thresholds ranging from  $k = 0$  mm to 20 mm are shown in Figure 3. Since the snow products were comprehensively used in watersheds hydrology, we estimate the accuracy based on the different sub-basins. The overall accuracy for different sub-basins changes for different thresholds. For all the sub-basins, the overall accuracy increases from  $k = 0$  mm to 5 mm, then reaches the highest overall accuracy about  $k = 6$  mm to 9 mm, then decreases after  $k = 10$  mm. The highest overall accuracy in the sub-basins varies from 91% to 94%, while the lowest overall accuracy varies from 87% to 90%. The Peel and Great Bear have the highest overall accuracy at about 94%, while the Peace has the lowest overall accuracy at about 91%. In addition, the Peel and Great Bear have the highest over-estimation errors and the lowest under-estimation errors; however, the Peace is the sub-basin with highest under-estimation errors and lowest over-estimation errors. Since land cover affects the passive microwave remotely sensed SWE significantly, the land cover in the different sub-basins was estimated from the 2004 MODIS International Geosphere-Biosphere Programme (IGBP) 1 km products (<http://edcdaac.usgs.gov/>). The land cover results show that the Peel and Great Bear are dominated by sparse forest (94%) and open area (80%), respectively; however, the other sub-basins are dominated by coniferous and deciduous forests, with fractions ranging from 50% to 75%. Owing to the effects of vegetation on microwave radiation from snow pack, the Peace sub-basin has the lowest overall accuracy and highest under-estimation errors.

Figure 3. (a) overall accuracy, (b) overestimation errors, and (c) underestimation errors of snow cover maps from different thresholds of AMSR-E L3 snow water equivalent in the sub-basins of the Mackenzie River Basin.



## 5. Conclusions and Discussion

This study used *in situ* SD observations and MODIS snow cover maps to evaluate the passive microwave remotely sensed SWE from AMSR-E and snow cover maps based on the SWE in the MRB, Canada. The comparison between *in situ* SWE and AMSR-E SWE showed that the mean absolute error ranges from 12 mm in the early winter to 50 mm in the late winter in the MRB. Ideally the best way to evaluate the accuracy of the AMSR-E SWE estimates is by comparing them with direct snow course measurements of SWE within AMSR-E pixels. However the poor temporal coverage of the available snow course measurements and the measurement cost significantly limit the use of those observations for evaluating the SWE algorithm. In this study, as no sufficient snow course measurements are available, we used daily SD derived SWE values. The SD derived SWE are themselves affected by errors, for example Derksen *et al.* [8] show that in winter 1992–1993 they explain only 63% of the variance of the observed SWE. Hence, the accuracy of the AMSR-E SWE products estimated in this study could potentially be higher (or lower), depending on the accuracy of the SD derived SWE. More direct SWE measurements are needed to clarify this issue.

Snow cover maps were produced based on the retrieved SWE from AMSR-E. The MOD10A2 snow maps were used as the reference data to evaluate the overall accuracy, under-estimation errors and over-estimate errors for the AMSR-E snow maps. MOD10A2 snow maps have been evaluated under different land cover and topography regions to a very high accuracy [4-6,16,17]. Errors in the MOD10A2 snow maps may impact the selected optimal SWE threshold,  $k$ , for a specific region. However the overall accuracy of the resulting AMSR-E snow maps may change or not. Still the accuracy of the final AMSR-E snow map products will benefit from selecting a specific SWE threshold in different regions. If the threshold of 1 mm is used to produce snow maps of AMSR-E, the SCE is over-estimated by 4% to 8% depending on the different land cover classes. The results showed that when a threshold of SWE  $k = 6$  mm to 9 mm, the overall accuracy of snow maps from AMSR-E reaches a maximum ranging from 91% to 94% for the different sub-basins. The sub-basin with the greatest proportion of forest cover, the Peace, had the lowest overall accuracy and highest under-estimation error, suggesting vegetation had a notable influence on the microwave radiation from the snow pack.

## Acknowledgements

This work is supported by grants from NASA's Cryospheric Science Program, Solid Earth and Natural Hazards Program, Terrestrial Hydrology Program. The authors also thank Ross Brown and Chris Derksen in Environment Canada for supplying the snow density data and their constructive comments. Comments by three anonymous referees greatly improved the paper.

## References

1. Yang, D.; Robinson, D.; Zhao, Y.; Estilow, T.; Ye, B. Streamflow response to seasonal snow cover extent changes in large Siberian watersheds. *J. Geophys. Res.* 2003, *108*, 4578, doi:10.1029/2002JD003149.



2. Yang, D.; Zhao, Y.; Armstrong, R.; Robinson, D. Streamflow response to seasonal snow cover mass changes over large Siberian watersheds. *J. Geophys. Res.* 2007, *112*, F02S22, doi: 10.1029/2006JF000518.
3. Brown, R.D. Northern hemisphere snow cover variability and change 1915–1997. *J. Climat.* 2000, *13*, 2339-2355.
4. Zhou, X.; Xie, H.; Hendrickx, M.H. Statistical evaluation of remotely sensed snow-cover products with constraints from streamflow and SNOTEL measurements. *Remote Sens. Environ.* 2005, *94*, 214-231.
5. Tong, J.; Déry, S.J.; Jackson, P.L. Topographic control of snow distribution in an alpine watershed of western Canada inferred from spatially-filtered MODIS snow products. *Hydrol. Earth Syst. Sci.* 2009a, *13*, 319-326.
6. Tong, J.; Déry, S.J.; Jackson, P.L. Interrelationships between MODIS/Terra remotely sensed snow cover and the hydrometeorology of the Quesnel River Basin, British Columbia, Canada. *Hydrol. Earth Syst. Sci.* 2009b, *13*, 1349-1452.
7. Tong, J.; Déry, S.J.; Jackson, P.L.; Derksen, C. Snow distribution from SSM/I and its relationships to the hydroclimatology of the Mackenzie River Basin, Canada. *Adv. Water Resour.* 2010, *33*, 667-677.
8. Derksen, C.; Walker, A.; Goodison, B. A comparison of 18 winter seasons of in situ and passive microwave-derived snow water equivalent estimates in Western Canada. *Remote Sens. Environ.* 2003, *88*, 271-282.
9. Derksen, C.; Walker, A.; Goodison, B. Evaluation of passive microwave snow water equivalent retrievals across the boreal forest/tundra transition of western Canada. *Remote Sens. Environ.* 2005, *96*, 315-327.
10. Tekeli, A.E. Early findings in comparison of AMSR-E/Aqua L3 global snow water equivalent EASE-grids data with *in situ* observations for Eastern Turkey. *Hydrol. Proc.* 2008, *22*, 2737-2747, doi: 10.1002/hyp.7093.
11. Brown, R.D.; Derksen, C.; Wang, L. Assessment of spring snow cover duration variability over northern Canada from satellite datasets. *Remote Sens. Environ.* 2007, *111*, 367-681.
12. Wang, L.B.; Sharp, M.; Brown, R.; Derksen, C.; Rivard, B. Evaluation of spring snow covered area depletion in the Canadian Arctic from NOAA snow charts. *Remote Sens. Environ.* 2005, *95*, 453-463.
13. Chang, A.T.C.; Foster, J.L.; Hall, D.K. Nimbus-7 SMMR derived global snow cover parameters. *Ann. Glaciol.* 1987, *9*, 39-44.
14. Chang, A.T.C.; Kelly, R.E.; Foster, J.L.; Hall, D.K. Global SWE monitoring using AMSR-E data. In *Proceedings of 2003 IEEE International Geoscience and Remote Sensing Symposium*, Toulouse, France, 21–25 July 2003; pp. 680-682.
15. Hall, D.K.; Riggs, G.A.; Salomonson, V.V.; Digirolamo, N.E.; Bayr, K.J. MODIS snow-cover products. *Remote Sens. Environ.* 2002, *83*, 181-194.
16. Hall, D.K.; Riggs, G.A. Accuracy assessment of the MODIS snow-cover products. *Hydrol. Proc.* 2007, *21*, 1534-1547.

17. Parajka, J.; Blöschl, G. Spatio-temporal combination of MODIS images-potential for snow cover mapping. *Water Resour. Res.* 2008, *44*, W03406, doi:10.1029/2007WR006204.

© 2010 by the authors; licensee MDPI, Basel, Switzerland. This article is an open access article distributed under the terms and conditions of the Creative Commons Attribution license (<http://creativecommons.org/licenses/by/3.0/>)